Received: 5 February 2023 | Revised: 20 April 2023 | Accepted: 23 April 2023

DOI: 10.1111/apha.13981

ACTA PHYSIOLOGICA

RESEARCH PAPER

Lack of the transcription factor *Nfix* causes tachycardia in mice sinus node and rats neonatal cardiomyocytes

Sara Landi[1] | **Federica Giannetti**[1] | **Patrizia Benzoni**[1] | **Giulia Campostrini**[1] | **Giuliana Rossi**[2] | **Chiara Piantoni**[1] | **Giorgia Bertoli**[1] | **Chiara Bonfanti**[2] | **Luca Carnevali**[1] | **Annalisa Bucchi**[1] | **Mirko Baruscotti**[1] | **Giorgia Careccia**[2] | **Graziella Messina**[2] | **Andrea Barbuti**[1]

[1]The Cell Physiology MiLab, Department of Biosciences, Università degli Studi di Milano, Milan, Italy

[2]Department of Biosciences, Università degli Studi di Milano, Milan, Italy

Correspondence
Andrea Barbuti, The Cell Physiology MiLab, Department of Biosciences, Università degli Studi di Milano, Milan, Italy.
Email: andrea.barbuti@unimi.it

Present address
Sara Landi, Human Technopole, Milan, Italy

Federica Giannetti, Center for Cardiac Arrhythmias of Genetic Origin and Laboratory of Cardiovascular Genetics, Istituto Auxologico Italiano IRCCS, Milan, Italy

Giulia Campostrini, Department of Anatomy and Embryology, Leiden University Medical Center, Leiden, The Netherlands

Giuliana Rossi, Roche Institute for Translational Bioengineering (ITB), Roche Pharmacy Research and Early Development Roche Innovation Center, Basel, Switzerland

Chiara Piantoni, Institute of Cardiovascular Physiology and Pathophysiology, Walter Brendel Center for Experimental Medicine, Biomedical Center (BMC), LMU München, Munich, Germany

Giorgia Bertoli, The Leon Charney Division of Cardiology, New York University Grossmann School of Medicine, New York, New York, USA

Luca Carnevali, Stress Physiology Lab, Department of Chemistry, Life Sciences and Environmental Sustainability, University of Parma, Parma, Italy

Funding information
European Research Council; French Muscular Dystrophy Association, Grant/Award Number: 20002

Abstract

Aims: *Nfix* is a transcription factor belonging to the *Nuclear Factor I* (NFI) family comprising four members (*Nfia*, *b*, *c*, *x*). *Nfix* plays important roles in the development and function of several organs. In muscle development, *Nfix* controls the switch from embryonic to fetal myogenesis by promoting fast twitching fibres. In the adult muscle, following injury, lack of *Nfix* impairs regeneration, inducing higher content of slow-twitching fibres. *Nfix* is expressed also in the heart, but its function has been never investigated before. We studied *Nfix* role in this organ.

Methods: Using *Nfix*-null and wild type (WT) mice we analyzed: (1) the expression pattern of *Nfix* during development by qPCR and (2) the functional alterations caused by its absence, by in vivo telemetry and in vitro patch clamp analysis.

Sara Landi and Federica Giannetti equally contributed to this work.

Results and Conclusions: *Nfix* expression start in the heart from E12.5. Adult hearts of *Nfix*-null mice show a hearts morphology and sarcomeric proteins expression similar to WT. However, *Nfix*-null animals show tachycardia that derives form an intrinsic higher beating rate of the sinus node (SAN). Molecular and functional analysis revealed that sinoatrial cells of *Nfix*-null mice express a significantly larger L-type calcium current (*Cacna1d* + *Cacna1c*). Interestingly, downregulation of *Nfix* by sh-RNA in primary cultures of neonatal rat ventricular cardiomyocytes induced a similar increase in their spontaneous beating rate and in I_{CaL} current. In conclusion, our data provide the first demonstration of a role of *Nfix* that, increasing the L-type calcium current, modulates heart rate.

KEYWORDS

ion channels, L-type calcium current, neonatal rat ventricular cardiomyocytes, Nfix, sinus node, tachycardia

1 | INTRODUCTION

Nfix is a transcription factor (TF) belonging to the *Nuclear Factor I* (NFI) family that includes also *Nfia*, *Nfib*, and *Nfic*.[1] *Nfix* is expressed in several tissues, both during development and in adulthood, but so far its role has been extensively studied only in the central and peripheral nervous system, in hematopoiesis and in the skeletal muscle.[1] In the developing muscle in particular, *Nfix* is involved in the secondary myogenesis where it induces the transcriptional switch from embryonic to fetal myogenesis. Moreover, *Nfix* plays also an important role in adult myogenesis as demonstrated by a delayed onset of muscle regeneration following acute injury, and by a higher content of slow-twitching fibre, in mice lacking *Nfix*.[2,3] Despite *Nfix* expression has been reported in the heart long ago,[4] its specific expression pattern and functional role in this organ has never been studied. The aim of this work has been to investigate the role of this TF in heart physiology using *Nfix*-null mice and their wild type (WT) littermates.

In the last decades, TFs specifically involved in the sinoatrial node (SAN) development and in the function of SAN cardiomyocytes have been identified (*Shox2*, *Tbx18*, *Tbx3*, *Isl-1*, *Gata6*).[5] In almost all cases, knockout of these genes cause early embryonic lethality (between E11.5 and 14.5) due to the lack of proper SAN development. Moreover, haploinsufficiency of these genes causes a significant bradycardia mostly due to a reduced pacemaker I_f current, caused by a decreased expression of HCN4 channels.[5] These genetic pathways are not species-specific, indeed Shox2 knockdown in zebrafish, although not lethal, induces downregulation in the SAN of Isl1 and HCN4 expression, and bradycardia.[6]

So far, TFs that modulate only the intrinsic heart rate of the adult SAN, without impairing its development are not known.

Here we analyzed the cardiac effect of knocking down the TF *Nfix*, important in skeletal muscle development and regeneration, whose expression in the heart was known since 1997 but whose role in this organ has never been addressed before. Nfix is not expressed at very early stages of heart development, before E12.5, when the heart has already adopted its four-chambered morphology. After E12.5 its expression raises steadily up to postnatal Day 5 when, in the whole heart, remains constantly expressed at similar levels up to adulthood. This suggests that *Nfix* may have a regulatory role on heart function rather than on its embryonic development. Differently from the knock down of the TFs described above, *Nfix*-null mice do not show any cardiac developmental defect but display a marked intrinsic SAN tachycardia due to a significantly larger L-type calcium current density. Also, we demonstrated that *Nfix* function, in modulating spontaneous beating rate, is conserved among species since its knockdown in spontaneously beating Neonatal Rat Ventricular Cardiomyocyte (NRVC) causes the same effects as in the mouse SAN (higher beating rate and increased L-type calcium current).

These data identify Nfix as a novel postnatal modulator of heart rate; *Nfix* expression appear to be normally lower in spontaneously beating cells (SAN cells and NRVC) and higher in quiescent working myocardium (atria and ventricles).

2 | MATERIALS AND METHODS

2.1 | Animals

Mice were kept in pathogen-free conditions; the day of the experiments mice were euthanized by cervical dislocation and the heart promptly removed. All the procedures conformed

to European and Italian laws (2010/63/UE D. and Lgs n. 2014/26) and were approved by the Animal Welfare Body of the Università degli Stud di Milano and by the Italian Minister of Health (protocol number 273/2018-PR).

Nfix-null and WT mice were generated crossing heterozygous *Nfix*-null+/− mice (C57 BL6/1295) obtained from Prof. Richard M. Gronostajski (University of Buffalo, NY, USA). To improve survival of *Nfix*-null mice, from postnatal Day 21 *Nfix*-null and control WT mice diet was supplemented with a soft dough chow (Transgenic Dough Diet, Bioserv), as previously described.[7]

2.2 | RNA extraction and retrotranscription

To isolate RNA from tissues, *RNAse*-free glass mortar, pestles, tubes, and sterile insulin needles were used to homogenize the sample in 1 mL of TRIzol® Reagent (Thermo Fisher). After the mechanical disruption of cell membranes, the sample was centrifuged at 12000 ×**g** for 5 min and the supernatant was transferred in a new *RNAse*-free tube to which 200 µL of Chloroform:Isoamyl alcohol 49:1 (Sigma Aldrich) was added; tubes were inverted and then incubated for 4 min at room temperature. Samples were centrifuged at 12000 ×**g** for 15 min at 4°C. The aqueous phase was transferred in a new RNAse-free tube in which 1 µL of 20 µg/mL Glycogen (Thermo Fisher) and 400 µL of Isopropanol (Sigma Aldrich) were added and gently inverted ten times. To facilitate RNA precipitation, samples were incubated for 10 min at room temperature and then centrifuged at 12000 ×**g** for 10 min at 4°C. The RNA pellet was washed three times in 1 mL of cold 75% Ethanol (Sigma Aldrich) and centrifuged at 7500 ×**g** for 5 min at 4°C. After discarding the supernatant and the complete evaporation of ethanol from the tube, the pellet was resuspended in MilliQ Water (Millipore-Sigma Aldrich) and incubated for 10 min at 60°C. Fresh isolated RNA was then stored at −80°C. RNA was quantified using Ultrospec® 500/1100 pro spectrophotometer (Amersham Biosciences). To eliminate residual genomic DNA, 1 µg of total RNA from each sample was treated with *DNAse I RNAse-Free* (Thermo Scientific) and incubated for 30 min at 37°C. To block DNAse I activity, 1 µL of 50 mM EDTA was added to the mixture and then incubated for 10 min at 65°C (Table 1). cDNA retrotranscription with random examers of DNAse-treated RNA was performed with the *cDNA Synthesis Kit for RT-qPCR* (Thermo Fisher) (Table 2) with the following temperature steps: 25°C for 10 min, 50°C for 15 min and 85°C for 5 min.

2.3 | qRT-PCR

Gene expression was quantified by real-time qPCR (Linegene 9600plus, Bioer); experiments were carried out using

TABLE 1 Primers sequences.

Gene	Forward primer 5′➔3′	Reverse primer 5′➔3′
mNfix	CTGGCTTACTTTGTCCACACT	CCAGCTCTGTCACATTCCAGA
mGapdh	AGGTCGGTGTGAACGGATTTG	TGTAGACCATGTAGTTGAGGTCA
mRps15a	AAACTGACGTGAAGGGAGCA	CCTCACAGGAAGGTTGAACAAG
mNkx2.5	GACGTAGCCTGGTGTCTCG	GTGTGGAATCCGTCGAAAGT
mMyh6	TGCTCAGAGCTCAAGAAGGAT	CCCAGCCATCTCCTCTGTTA
mMyh7	CAGCAGACTCTGGAGGCTCTT	AGGGCGACCTCAACGAGAT
mMlc2v	GGACACATTTGCTGCCCTA	ATCGTGAGGAACACGGTGA
mTnI	GCAGGTGAAGAAGGAGGACA	CGATATTCTTGCGCCAGTC
mCacna1c	TAGTGTCCGGAGTCCCAAGT	GAAGAGCACAAGAAGGGCAAT
mCacna1d	GTTGTAAGTGCGGTAGAAAGCA	CTGGTGCCTCTTGCATAGTTT
mCacna1g	TAACCTGCTTGTCGCCATT	ACTCGTATCTTCCCGTTTGC
mCacna1h	CCTGCTGGACACTGTGGTT	GGAGCATGAAAAGAAGACCAA
mHCN1	CTCAGTCTCTTGCGGTTATTACG	TGGCGAGGTCATAGGTCAT
mHCN2	CCGCTGTTTGCCAATGC	AGGCTGGAAGACCTCAAATTTG
mHCN4	GTCGGGTGTCAGGCGGGA	GTGGGGGCCACCTGCTAT
rNfix	CTGGCTTACTTTGTCCACACT	CCAGCTCTGTCACGTTCCAGAC
rGapdh	GATTTGGCCGTATCGGAC	GAAGACGCCAGTAGACTC

Note: All primer pairs were tested for an efficiency >95%.

Abbreviations: m = *Mus musculus*, r = *Rattus norvegicus*.

TABLE 2 Action potential parameters analyzed in SAN cardiomyocytes.

SAN cells	WT, $n=10$	*Nfix*-null, $n=10$
RATE (bpm)	412.9 ± 46.8	585.0 ± 36*
MDP (mV)	−61.0 ± 2.1	−58.5 ± 2.6
APA (mV)	91.6 ± 7.2	85.0 ± 5.9
APD50c (ms)	64.5 ± 4.8	70.0 ± 5.6

*$p < 0.05$.

Maxima SYBR Green/ROX qPCR Master Mix (Thermo Scientific) qPCR conditions were 95°C for 5 min, followed by 45 cycles at 95°C for 15 s, 60°C for 30 s, and 72°C for 30 s. The melting curve analysis (60–96°C) was performed at the end of the protocol to verify the presence of a single amplicon. Each sample was run in triplicate and the mean cycle threshold (Ct) of the gene of interest (GOI) was normalized to the mean Ct of the housekeeping (HSK) gene (Gapdh or Rps15a). The data are displayed as $2^{-\Delta Ct}$*100, considering $\Delta Ct = Ct_{GOI} - Ct_{HSK}$.

2.3.1 | Histological analysis

Hearts were blocked in diastole using 100 μM $CdCl_2$ (Sigma Aldrich) and immediately fixed in 4% PFA (Sigma Aldrich). Excess of fixative was removed with two washes with PBS (Sigma Aldrich) of 5 min each under gentle shaking. Samples were successively re-equilibrated in PBS-sucrose solutions at increasing sucrose concentrations: 1 h with 7.5% sucrose, 1 h with 15% sucrose, and O/N in 30% sucrose, at 4°C under constant shaking. The day after, samples were embedded in OCT (Bio-Optica), included in nitrogen-cooled isopentane (VWR), and maintained at −80°C until further processing. For Hematoxylin and Eosin and Milligan's Trichrome stainings, 7 μm sections were cut with a cryostat (Leica) on positively charged glass slides (Superfrost Plus, Thermo Scientific). Sections were stained with hematoxylin and eosin (Sigma Aldrich) according to standard protocols. Briefly, samples were washed in distilled water and stained with hematoxylin for 4 min. Excess of staining was removed with a 15 min wash under running water, then slices were progressively dehydrated to 90% Ethanol (VWR) and stained for 7 min with 0.5% Eosin in 90% Ethanol. Slices were then further dehydrated through successive steps in graded alcohol solutions, cleared with xylene (VWR) and mounted with Eukitt mounting medium (Bio-Optica). For Milligan's trichrome, sections were fixed for 1 h with Bouin's fixative (Sigma Aldrich) and rinsed for 1 h under running water. Sections were then rapidly dehydrated to 95% Ethanol in graded ethanol solutions; successively they were passed in 3% potassium dichromate (Sigma Aldrich) for 5 min and rapidly washed in distilled water. Then, samples were stained with 0.1% acid fuchsin (Sigma Aldrich) for 30 s, washed again in distilled water and passed in 1% phosphomolybdic acid (Sigma Aldrich) for 3 min. After, they were stained with Orange G (2% in 1% phosphomolybdic acid) (Sigma Aldrich) for 5 min, rinsed in distilled water, passed in 1% acetic acid (VWR) for 2 min, stained with 1% Fast Green for 5 min (Sigma-Aldrich), passed in 1% acetic acid for 3 min, rapidly dehydrated to 100% Ethanol and cleared in Xylene before mounting with Eukitt (Bio-Optica). Images were acquired with a Leica-DMI6000B microscope equipped with a 10× magnification objective. Leica DFC400 camera was used for image capture.

2.3.2 | In vivo telemetry

3–6 month-old mice were implanted with a radio frequency transmitter (*TA10ETA-F20*, *DSI*) as previously described.[8] Briefly, mice were anesthetized by inhalation of 5% isoflurane (Isoflurane-VET, Merial) in 100% oxygen and maintained at 1.5%–3% isoflurane in 100% oxygen at a flow rate of 1 L/min. Before surgery and for 5 days after, mice received the analgesic Rymadil (5 mg/kg, Pfizer) and the antibiotic Baytril (5.8 mg/kg, Bayer). A radio-transmitter (ETA-F10, Data Sciences Int.) was implanted for the simultaneous recordings of cardiac rate (sampling frequency 2000 Hz), activity and temperature in freely moving conditions, as previously reported.[9] After surgery, animals were housed individually and allowed to recover for 15 days before starting data collection. Data were acquired by Dataquest A.R.T. (TM) Gold 4.3. ECG signals were recorded by platform receivers (RPC-1, Data Sciences Int.) for 120 s every 30 min for five consecutive days, with the animals left undisturbed and free to move in their cages. ECG signals were recorded and acquired via Dataquest A.R.T. (TM) Gold 4.3 acquisition system (Data Sciences Int.).

For the analysis, each 2 min raw ECG signal was visually inspected to ensure that all R-waves were correctly detected. Those parts of ECG recordings which exhibited recording artifacts were discarded without substitution and excluded from further analysis. Heart rate (reported in beats per minute, bpm) was extrapolated from R-R waves distance using ChartPro 5.0 software (ADInstruments).

Initially, separate calculation of HR was done for each 2-min recording period and subsequently averaged as mean values of the 12 h-light and 12 h-dark phase of each recording day. These parameters were then further averaged to obtain the final mean rate values for light and dark phases.

Data were collected as 2-min recording period every 30 min. For each mouse, these data were then averaged as mean value for every day of recording. The values reported in the paper indicates the number of mean values obtained from the 5 days of recordings (Day 1 + Day 2 + Day 3 + Day 4 + Day 5) vs. the number of mice used for the study (5 WT mice vs. 4 Nfix null mice). Not all the mice enrolled in the study survived to 5 days of telemetry, especially in the case of *Nfix*-null mice. This explains why, for example, you would expect from *Nfix*-null a total of 20 points instead of 18/17 (4 mice × 5 days = 20 mean values).

2.4 | Isolation of sinoatrial node (SAN) cells

SAN cells (SANCs) were isolated from 4–6-month-old *Nfix*-null and WT mice (both males and females) as previously described.[10] Hearts were explanted and put immediately in Tyrode's's solution (mM: 140 NaCl, 5.4 KCl, 1.8 $CaCl_2$, 1 $MgCl_2$, 5.5 D-glucose, 5 Hepes-NaOH; pH 7.4) plus 1000 U Eparin. During the SAN dissection, the tissue was maintained in warm (37°C) Tyrode's and placed onto the stage of a stereomicroscope. The tissue is then cut in four to five pieces and immediately washed for three times in a low-calcium solution (mM: NaCl 140, KCl 5.4, $MgCl_2$ 0.5, KH_2PO_4 1.2, HEPES-NaOH 5, Taurine 50, D-glucose 5.5; pH = 6.9) for 1 min. Then, SAN was enzymatically digested for at least 25 min at 37°C using low-calcium solution plus 0.2 mM $CaCl_2$, 1 mg/mL BSA, 0.45 U/mL Protease (Sigma Aldrich), 1.30 U/mL Elastase (Sigma Aldrich) and 250 U/mL Collagenase IV (Worthington). Once the enzymatic incubation was over, the SAN pieces were washed three times in zero-calcium solution (mM: KOH 80, L-Glutamic Acid 70, KCl 20, βOH-butyric acid 10, KH_2PO_4 10, HEPES-KOH 10, Taurine 10, EGTA-KOH 1; 1 mg/mL BSA, pH = 7.4) and then mechanically digested for 10 min. Cells were then gradually adapted to physiological calcium concentrations using the following steps every 4 min at 4°C:

1. +72 μL of a solution containing 10 mM NaCl and 1.8 $CaCl_2$;
2. +153.6 μL of a solution containing 10 mM NaCl and 1.8 $CaCl_2$;
3. +374.4 μL of Tyrode's plus 1 mg/mL BSA;
4. +1200 μL of Tyrode's plus 1 mg/mL BSA;
5. +4200 μL of Tyrode's plus 1 mg/mL BSA;

At the end of the protocol, SANCs were plated in the center of 35-mm Petri dishes and maintained at 4°C for the day of the experiment.

2.5 | Isolation and infection of neonatal rat ventricular cardiomyocytes

Primary cultures of NRVCs were prepared as previously described.[11] 24 h after NRVC isolation, 10^6 cells were infected with a lentivirus carrying the vector plKO.1 with either a scrambled hairpin sequence (Scramble) or a short hairpin RNA specific for downregulating *Nfix*-mRNA (*Nfix*-sh) and a puromycin resistance cassette in the presence of Polybrene 4 μg/mL with a final multiplicity of infection (MOI) of 50.

After 24 h from the infection, cells were washed twice in PBS (Sigma Aldrich) and put under stringent 2 μg/mL puromycin selection. After 2 days of selection, only the infected, polybrene-treated cells survived. To evaluate infection efficiency for each experiment, two cell culture dishes of Polybrene-treated, non-infected NRVCs were used as controls:—*Negative CTRL* in which it was added puromycin to confirm induction of cell death;—*Positive CTRL* as a control between Scramble and not-infected NRVCs. Two days before electrophysiological recordings, infected NRVCs were dissociated into single cells by incubation for 2–3 min with Trypsin–EDTA (Sigma Aldrich) at 37°C and centrifuged at 300 ×***g*** for 5 min.

2.5.1 | Electrophysiology

For electrophysiology, cells were placed onto the stage of an inverted microscope and superfused with Tyrode's solution containing (mM): 140 NaCl, 5.4 KCl, 1.8 $CaCl_2$, 1 $MgCl_2$, 5.5 D-glucose, 5 Hepes-NaOH; pH 7.4. Patch-clamp pipettes had resistances of 3–6 MΩ when filled with the intracellular-like solution containing (mM): 130 K^+-aspartate, 10 NaCl, 5 EGTA-KOH, 2 $CaCl_2$, 2 $MgCl_2$, 2 ATP (Na^+-salt), 5 creatine phosphate, 0.1 GTP (Na^+-salt), 10 Hepes-KOH; pH 7.2. Temperature was kept at 36 ± 1°C. Spontaneous action potentials were recorded from either single cells or aggregates of few cells in current-clamp mode using the whole-cell configuration. Action potentials rate, action potential duration at 50% of repolarization (APD50), maximum diastolic potential (MDP) and the amplitude (APA) of the action potentials were analyzed. Since *Nfix*-null SAN cells have a higher rate, APD50 has been corrected for rate differences using Bazett's formula normally used for QT correction ($APD50c = APD50\sqrt{(RR)}$) where RR is the inter-beat-interval in ms. For voltage-clamp recordings only single cells were used. To dissect funny current (I_f) 1 mM $BaCl_2$ and 2 mM $MnCl_2$ were added to the Tyrode's. I_f was activated by hyperpolarizing voltage steps to the range −35 to −125 mV from a holding potential (hp) of −30 mV. Each step was long enough to reach steady-state current activation. Activation curves

were obtained from normalized tail currents measured at −125 mV and fitted to the Boltzmann distribution: $y=(1/(1+\exp(V-V_{1/2})/s))$, where V is voltage, y fractional activation, $V_{1/2}$ the half-activation voltage, and s the inverse-slope factor. For L-type calcium current (I_{CaL}) recordings, we used an extracellular solution containing (mM): CsCl 10, NaCl 135, $CaCl_2$ 1, $MgCl_2$ 1, HEPES 5, Glucose 11.1, Tetrodotoxin (TTX) 0.03, pH = 7.4; I_{CaL} was activated by depolarizing voltage steps in the range −70 to +50 mV of 200 ms duration, from a hp of −80 mV. To specifically block I_{CaL}, 10 μM Nifedipine was added. I_{CaL} was considered as the Nifedipine-sensitive component. Conductance was calculated by fitting to a straight line the ohmic part of the *I–V* curve.

2.6 | Statistical analysis

All the data are displayed as mean ± standard error of the mean. Either Student's *t*-test for normally distributed independent populations or one-way ANOVA for groups, followed by pairwise comparison using Fisher's test was used to test significance; $p < 0.05$ defines statistical significance.

3 | RESULTS

3.1 | Nfix is expressed during late cardiac development and in the adult heart

We first analyzed the cardiac expression of *Nfix* during murine cardiac development (E10.5–16.5), in the first week after birth (P1–P7) and in the adult ventricles (AV). Figure 1A shows the time course of *Nfix* mRNA expression in the heart from mid-gestation to adulthood. *Nfix* transcript is not expressed at E10.5, its expression increases linearly starting from E12.5, reaches a plateau in the first postnatal week, remaining then constant up to adulthood. In the adult heart, *Nfix* is expressed in both atria and ventricles, at levels similar to those of tibialis muscle and hippocampus, tissues known for their high *Nfix* expression (Figure 1B).

3.2 | The absence of *Nfix* does not influence the morphological characteristics of the heart

In order to evaluate a role of *Nfix* in cardiac morphology and physiology, we investigated the heart morphology of *Nfix*-null and WT mice. Histological analysis was performed on fixed heart sections obtained from 3-month-old *Nfix*-null and WT mice. Sections were stained with either Hematoxylin and Eosin or Milligan's Trichrome to highlight the presence of necrosis, hypertrophy, or fibrosis. No evident morphological differences between *Nfix*-null and WT hearts emerged, suggesting that the structure of the heart is normal in the absence of *Nfix* (Figure 2A). We also evaluated the expression of the other *Nfi* gene (Nfia-c) in atria and ventricles of both WT and *Nfix*-null mice. No alterations in the expression levels of any of these genes were found, with the expected lack of *Nfix* expression in the *Nfix*-null atria and ventricles (Figure 2B). Since *Nfix* plays a pivotal role in the organization of skeletal muscle

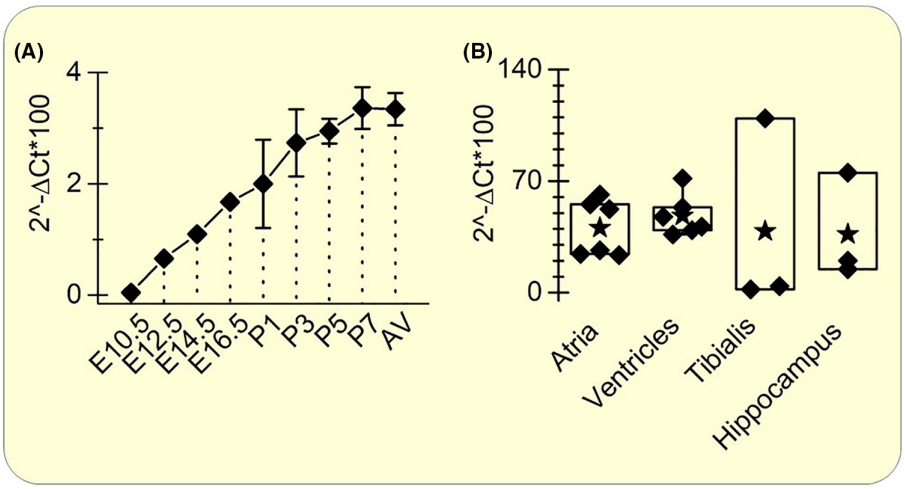

FIGURE 1 Nfix expression during heart development and in atria and ventricles of adult hearts. (A) Time course of Nfix mRNA expression by qPCR during heart development; To obtain detectable amounts of RNA during embryogenesis, different hearts samples were pulled together at each time point (E10.5 and E12.5: $N=6$; E14.5 and 16.5: $N=4$) postnatal day P1: $N=3$; P3: $N=4$; P5: $N=4$; P7: $N=4$; AV, $N=6$) (E = embryonic day; P = postnatal day; AV = adult ventricles). (B) Comparison of Mean Nfix expression levels in atria, ventricles, *tibialis anterior* muscle and hippocampus. Black stars represent mean values.

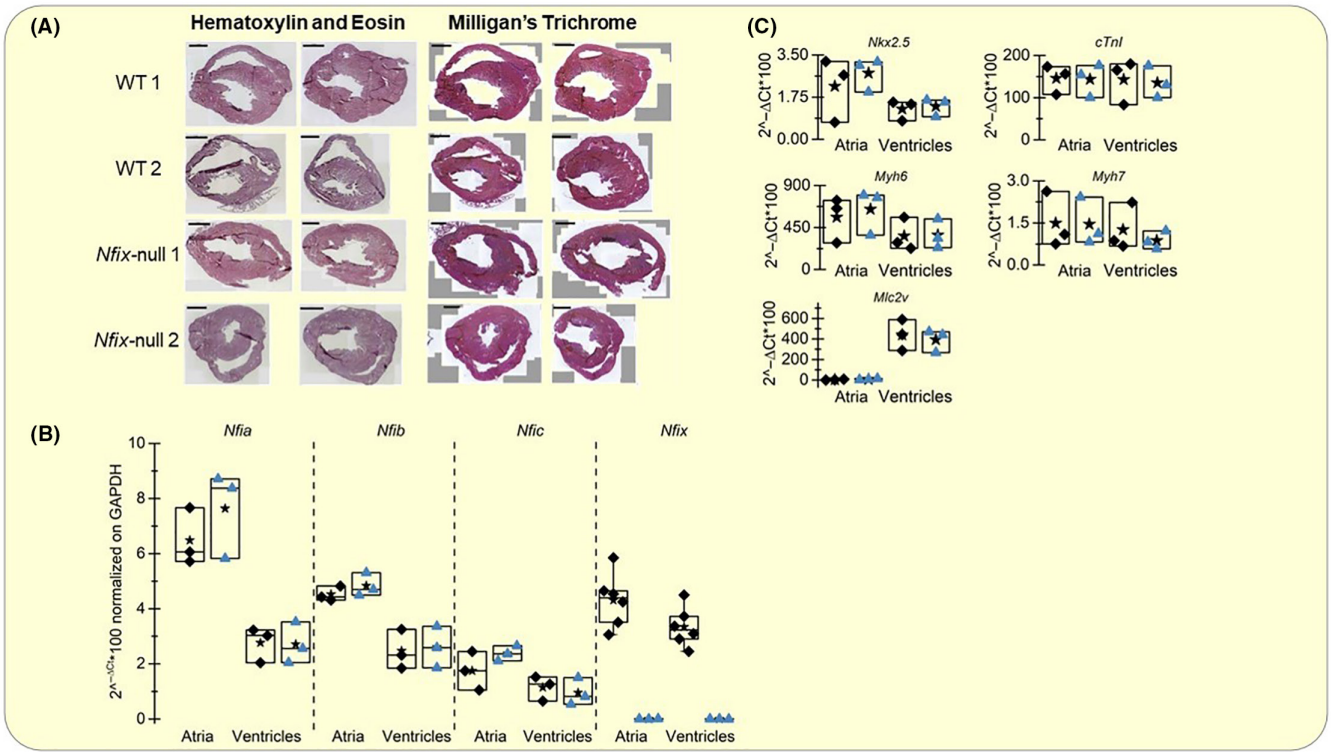

FIGURE 2 Morphological and molecular comparison of wild type (WT) and *Nfix*-null hearts. (A) Histological sections of two WT and two *Nfix*-null hearts by hematoxylin/eosin and Milligan's trichrome staining. Calibration bar = 1 mm. (B) Comparison of the expression levels of the four Nfi genes by qPCR, in WT (black diamonds) and Nfix-null (blue triangles) atria and ventricles of adult mice; each dot represents an independent biological replicate. (C) Comparison of the expression levels of the cardiac transcription factor Nkx2.5 and of the sarcomeric genes cTnI, Myh6, Myh7, Mlc2V and by qPCR, in WT (black diamonds) and *Nfix*-null (blue triangles) atria and ventricles. Black stars represent mean values.

sarcomeres and affecting myosin isoform expression,[2] alterations of myocardium-specific genes were investigated by qPCR in atria and ventricles of adult WT and *Nfix*-null mice. We considered the expression of the sarcomeric genes: cardiac troponin I (*cTnI*), cardiac-relevant myosin isoforms (*Mlc2v*, *Myh6*, and *Myh7*) and of the cardiac TF *Nkx2.5*. As shown in Figure 2C no statistically significant differences between the expression values of these genes in both atria and ventricles of *Nfix-null* and WT mice were found, suggesting that sarcomeric structural genes are not affected by the lack of *Nfix*.

3.2.1 | Lack of Nfix influences the heart rate

We then evaluated the effects of the absence of *Nfix* on the cardiac function; 3–6-month-old WT and *Nfix*-null mice were implanted with a radio transmitter and ECGs were recorded in freely moving conditions for 5 days. In Figure 3A, representative traces of ECGs recorded both during night (dark) and day (light) from WT and *Nfix*-null mice are shown, in which tachycardia of *Nfix*-null animals is clearly visible. Average data depicted in Figure 3B,C show that, as expected, heart rate significantly varies from night to day but *Nfix*-null mice maintain a significantly higher heart rate than WT both during dark (WT: 496.7 ± 13.17 bpm, $n = 22/5$; *Nfix*-null: 587.5 ± 8.7 bpm, $n = 18/4$) and light hours (WT: 467.0 ± 8.4 bpm, $n = 24/5$; *Nfix*-null: 523.1 ± 13.2 bpm, $n = 17/4$).

To understand if the in vivo tachycardia is intrinsic to the pacemaker tissue or may be due to an alteration in sympathovagal balance, pacemaker cells from the SAN were isolated for in vitro electrophysiological experiments. First, we evaluated *Nfix* expression in the SAN, the region responsible for the generation and modulation of heart rate.[12] As shown in Figure 3D *Nfix* is expressed in the SAN of WT mice and, as expected, it is absent in *Nfix*-null SAN. Representative action potentials traces recorded from WT and *Nfix*-null SAN cells are depicted in Figure 3E. Similarly to in vivo ECG data, *Nfix*-null SAN cells exhibit a significantly higher firing rate (585 ± 37 bpm, $n = 10$, $p = 0.05$) than WT-SAN cells (413 ± 47 bpm, $n = 10$) demonstrating that the in vivo tachycardia is an intrinsic characteristic of the SAN (sinus tachycardia), and thus independent from

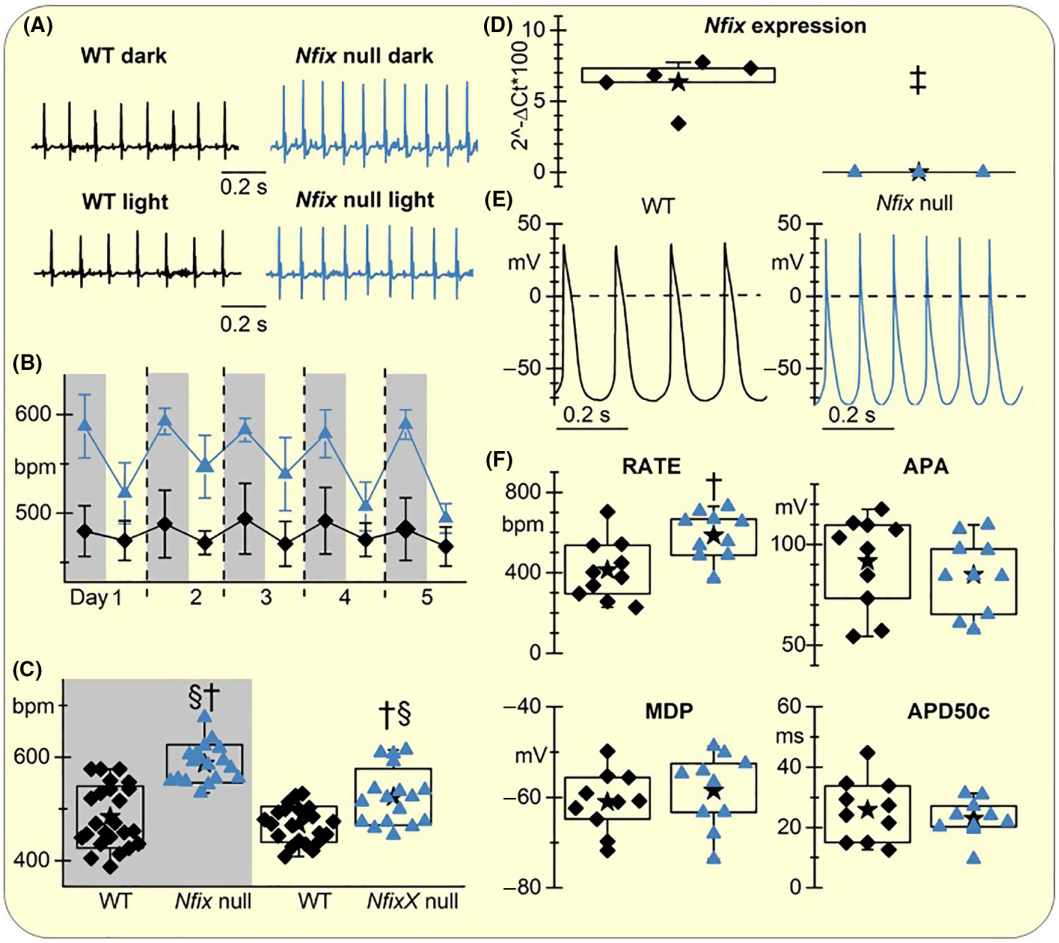

FIGURE 3 *Nfix*-null mice show sinus tachycardia. (A) Representative ECGs traces recorded from freely moving wild type (WT) and *Nfix*-null mice under dark (upper traces) and light (lower traces) conditions. (B) Time course of mean heart rate of WT (black diamonds) and *Nfix*-null mice (blue triangles) during the 5 days of recordings (dark, gray background; light, no background). (C) Box plot of the heart rate in WT and *Nfix*-null mice during night (gray background) and day (no background); each dot represents the mean heart rate of various recording throughout the day, in different animals (†$p < 0.05$ WT vs. Nfix-null; §$p < 0.05$ night vs. day). (D) Box plots of the expression levels of Nfix mRNA in the SAN of WT and Nfix-null mice. Each dot represents an independent biological replicate (‡$p < 0.001$). (E) Representative spontaneous action potentials recorded from isolated SAN cells of both animal groups. (F) Comparison of AP parameters: rate, APA (action potential amplitude), MDP (maximum diastolic potential), APD50 (action potential duration at 50% repolarization). Throughout the figure, black diamonds represent WT and blue triangles *Nfix*-null mice; the black star indicates the mean value (†$p < 0.05$).

the autonomic tone (Figure 3E). Beside rate, the other AP parameters, APA, MDP and rat-corrected action potential duration at 50% of repolarization (APD50c) did not show any significant difference between *Nfix*-null and WT-SAN cells (Figure 3F; Table 2).

It is interesting to note that a comparison of expression levels of *Nfix* in the various cardiac regions (atria, ventricles and SAN) highlights that *Nfix* mRNA is expressed in the atria and ventricles at levels comparable to those found in the skeletal muscle and hippocampus where it is known to be highly expressed,[1] while it is significantly less expressed in the SAN (cf. Figures 1B, 3D and Table 3) and also in beating NRVCs (see Figure 6A below). As expected, the transcript is not detected in any cardiac region from *Nfix*-null animals (Figures 2B and 3D).

TABLE 3 Comparison of Nfix expression levels in cardiac cells.

	$2^{-\Delta ct}*100$ (mean ± SEM)
Atria	40.6 ± 7.2
Ventricles	48.4 ± 5.3
SAN	6.3 ± 0.7*
NRVC	2.6 ± 0.6*

*$p < 0.001$ versus adult atria and ventricles.

3.3 | Functional mechanism of sinus tachycardia in *Nfix* null mice

Action potential firing originates from a combination of pacemaker currents involved during the diastolic

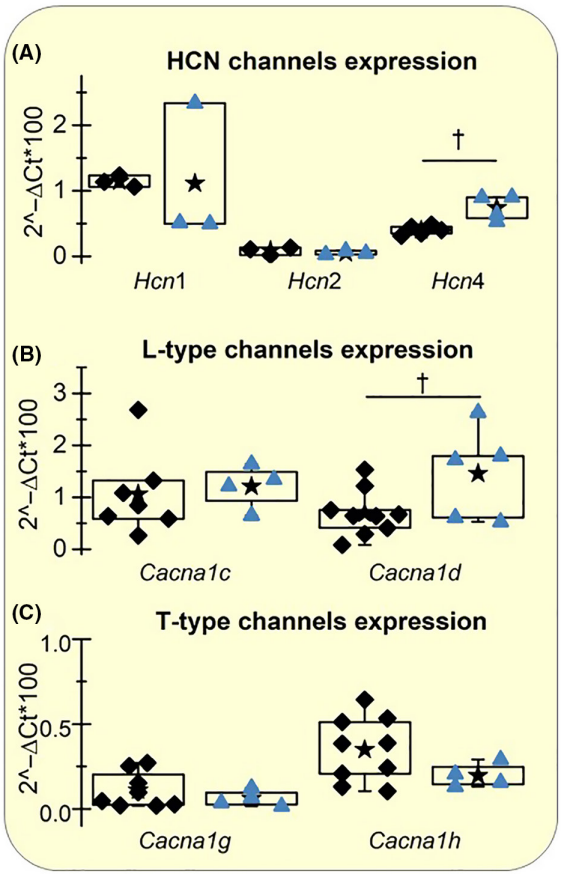

FIGURE 4 Expression levels of Hcn and Cacna1 genes in wild type (WT) and *Nfix*-null SAN. Box plots of the expression levels of f-channels (Hcn1, 2 and 4—A), L-type (Cacna1c and Cacna1d—B) and T-type (Cacna1g and Cacna1h—C) calcium channels, as indicated, in WT (black diamonds) and Nfix-null mice (blue triangles). †$p < 0.05$. The black stars indicate the mean values.

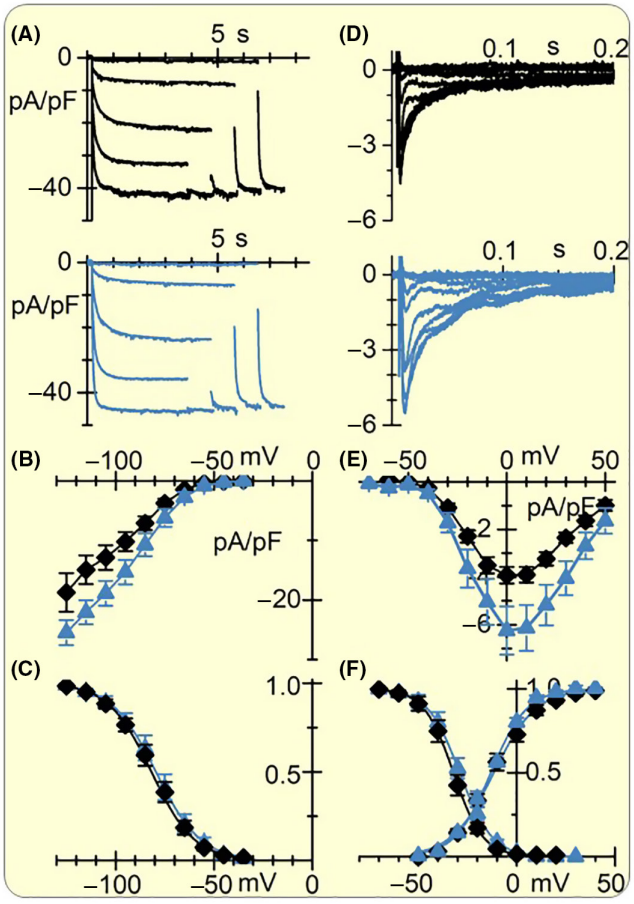

FIGURE 5 I_f and I_{CaL} currents in wild type (WT) and Nfix-null SAN cells. Representative traces of I_f (A) and Nifedipine-sensitive I_{CaL} (D) in WT (top, Black) and Nfix-null (bottom, blue) SAN cells. (B) Mean I_f *I–V* curve of WT (Black diamonds) and Nfix-null (blue triangles). (C) Mean I_f AC curves (symbols as in B). (E) Mean I_{CaL} *I–V* curves of WT (Black diamonds) and Nfix-null (blue triangles). (F) Mean I_{CaL} AC and IC curves (symbols as in B).

depolarization phase in which the funny current (I_f) and L-type calcium current (I_{CaL}) play pivotal roles.[8,13–15] To unravel the mechanism(s) at the basis of the sinus tachycardia observed in *Nfix*-null mice, we next evaluated the expression levels of the *Hcn* genes (*Hcn*1, *Hcn*2, and *Hcn*4) and of the L- and T-type calcium channels expressed in mouse SAN (*Cacna1c*, *1d*, *1g* and *1h*, respectively). Figure 4 shows that *Nfix*-null SAN express significantly higher levels of *Hcn*4 and *Cacna1d* subunits while the other genes analyzed were expressed at similar levels.

3.4 | *Nfix* loss does not affect the funny current I_f but enhances L-type calcium current

Since it has been reported that mRNA expression levels do not always correlate with ion current densities recorded in SAN cells,[16,17] we next evaluated the density and kinetic properties of the I_f and I_{CaL} in isolated SAN cells.

We did not find significant differences neither in conductance nor in the activation curves parameters of I_f (Figure 5A–C and Table 4). Instead, we found a significantly increased I_{CaL} conductance (Figure 5D,E) in *Nfix*-null SAN cells, without changes in both activation and inactivation parameters (Figure 5F, for values see Table 4).

3.5 | *Nfix*-silencing in NRVCs

Since many *Nfix*-null mice die during the first 3 weeks of life due to still poorly understood mechanisms, affecting initial stages of organs development,[7] the effects of *Nfix* loss on beating rate and ion currents were evaluated using another in vitro cellular model: primary cultures of spontaneously beating NRVCs. NRVC were infected with a lentivirus carrying either a short hairpin for silencing *Nfix* (sh-*Nfix*) or a scrambled sequence (SCR). Using

TABLE 4 I_{CaL} and I_f conductance and kinetic parameters analyzed in SAN cardiomyocytes.

SAN cells	I_{CaL} current		I_f current	
	WT, $n=17$	*Nfix*-null, $n=10$	WT, $n=15$	*Nfix*-null, $n=8$
g (pS/pF)	79.8 ± 7.0	113.2 ± 15.1*	163.1 ± 25.8	235.9 ± 20.9
AC $V_{1/2}$, k (mV)	−12.5 ± 1.5 mV, 9.3 ± 0.5 mV	−13.7 ± 1.4, 8.5 ± 0.5	−80.4 ± 2.4,9.3 ± 0.7	−79.6 ± 3.3, 9.9 ± 0.7
IC $V_{1/2}$,k, (mV)	−29.9 ± 1.3, 6.2 ± 6.2	−29.6 ± 2.1, 7.6 ± 7.5*		

*$p < 0.05$.

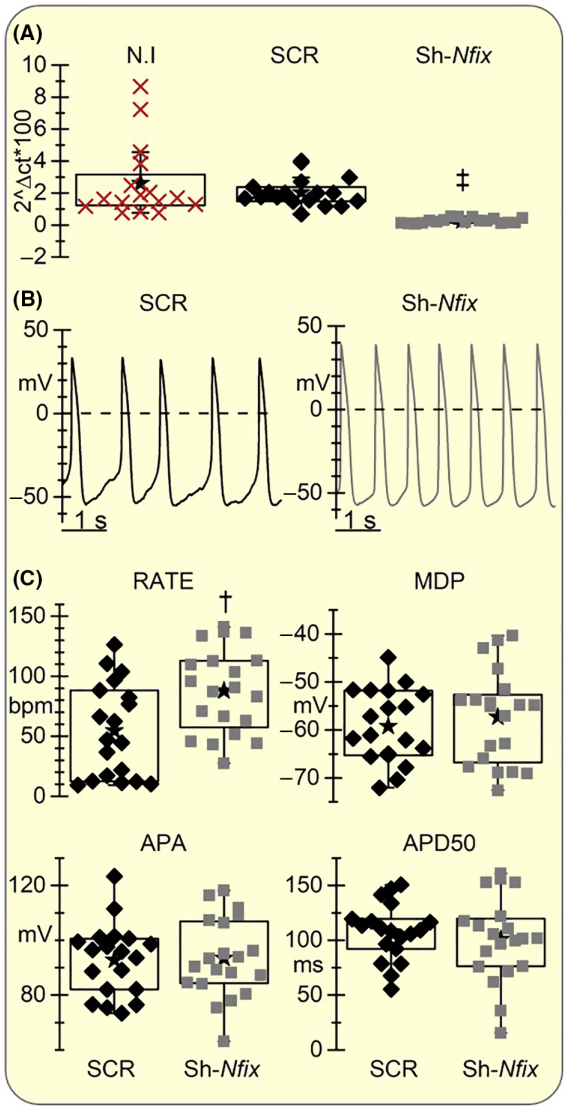

FIGURE 6 Rate and AP parameters in SCR and Nfix-sh infected Neonatal Ventricular Cardiomyocytes (NRVCs). (A) Mean Nfix-transcript expression in Non-infected (N.I, red X), Scramble (SCR, black diamonds) and Sh-Nfix NRVCs (gray squares); ANOVA Fisher's LSD, ‡$p < 0.001$. (B) Spontaneous action potentials recording from SCR and Nfix-sh NRVCs. (C) Boxplot of APs parameters in SCR (black diamonds) and Sh-Nfix (gray squares) NRVCs; The black stars indicate the mean values. Student's *t*-test, †$p < 0.05$.

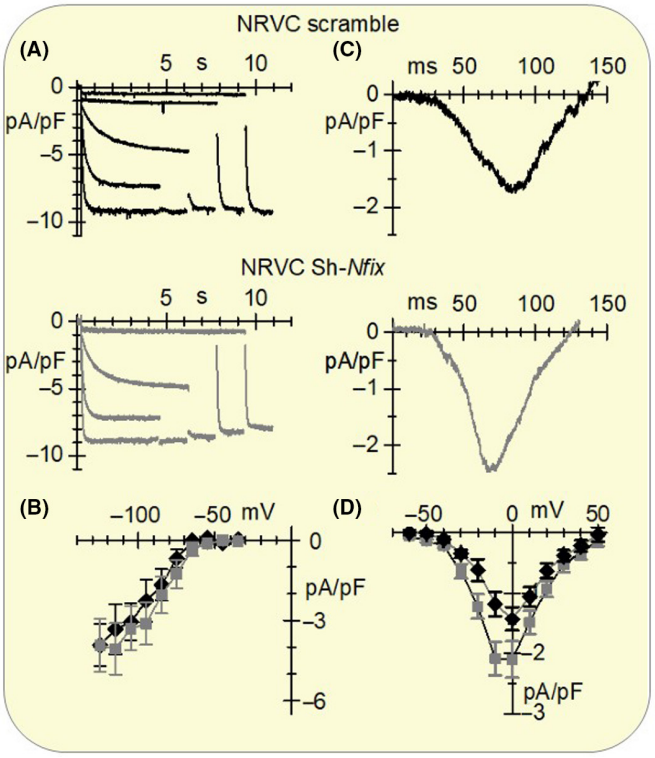

FIGURE 7 I_f and I_{CaL} currents in WT and Nfix-sh NRVC. Representative traces of I_f (A) and Nifedipine-sensitive I_{CaL} (C) in SCR (top, black) and Sh-Nfix (bottom, gray). (B) Mean I_f *I–V* curve of SCR (black diamonds) and Nfix-sh (gray squares). (D) Mean I_{CaL} *I–V* curves of SCR and Sh-Nfix (symbols as in B).

non-infected (N.I) and scramble-infected NRVCs as a control, we demonstrated that sh-*Nfix* infection caused a downregulation of 85.2% ± 2% ($n=18$) of the *Nfix* mRNA (Figure 6A). Representative traces of spontaneous action potentials recorded from both SCR- and sh-*Nfix* NRVCs are shown in Figure 6B. In agreement with data on SAN cells, sh-*Nfix* NRVCs displayed a higher action potential firing rate (87.8 ± 7.9 bpm†, $n=20$) than Scramble cells (54.5 ± 9 bpm, $n=19$). Again, no differences in APA, MDP, and APD50 were found (Figure 6C).

Finally, we evaluated the I_f and I_{CaL} currents in SCR and *sh-Nfix* NRVCs. Figure 7A,C displays representative traces of both currents from SCR (top, black) and sh-*Nfix* (middle, gray) NRVCs. Mean data (Figure 7B) confirm that, as in SAN cells, the I_f current did not differ between SCR and sh-*Nfix* NRVCs while I_{CaL} was significantly up-regulated in sh-*Nfix* NRVCs (Figure 7D). For values see Tables 5 and 6.

4 | DISCUSSION

The Nfi TF family includes four members, which have been shown to play important roles for the development of multiple organs.[18] *Nfix* expression is particularly abundant in skeletal muscle and brain and the functional roles of *Nfix* in development and physiology of these two tissues have been previously well characterized.[1–3] Interestingly, although Nfix expression in the heart has been reported more than 25 years ago,[4] its role in either cardiac development or function has not been assessed before.

Here, we investigated, for the first time, the role of *Nfix* during heart development and in adult heart morphology and function, comparing data collected from *Nfix*-null mice and WT littermates. We further extended our analysis using primary cultures of neonatal ventricular cardiac myocytes in which *Nfix* has been significantly downregulated (>80%) by viral infection using a specific shRNA (Sh-*Nfix*). In skeletal muscle *Nfix* is not expressed in embryonic muscles (E11.5) but starts to be highly expressed in fetal muscles (at E16.5). At the onset of fetal myogenesis, here *Nfix* drives the switch from an embryonic to a fetal myofiber phenotype by both promoting transcription of specific fetal genes (MCK and β-enolase) and repressing embryonic ones (slow myosin heavy chain).

In the heart, *Nfix* mRNA was not detectable at E10.5 and starting from E12.5 its expression increases linearly up to postnatal Day 5 when remains stable up to adulthood. Chaudhry et al. reported that *Nfix* mRNA levels were high in skeletal muscle and intermediate in hippocampus and heart.[4] Our qPCR data show instead similar *Nfix* mRNA levels in atria, ventricles, *Tibialis Anterior* muscle, and hippocampus.

Differently from what happens in skeletal muscle, morphological analysis did not revealed any difference in either heart morphology or dimension between adult WT and *Nfix*-null mice. Since in skeletal muscles *Nfix* is involved in the switch between embryonic and fetal myosin,[2] we evaluated the expression of cardiac myosin heavy chains *Myh7* and *Myh6*, predominantly expressed in the embryonic and adult mouse heart, respectively. No differences in their expression were induced by the lack of *Nfix*; the same holds true for other sarcomeric proteins (cTnT, Mlc2V) and for Nkx2.5, a TF important in heart development.[19] It is known that the other members of the *Nfi* family are expressed together with *Nfix* during development. However, Nfia, Nfib, and Nfic were similarly expressed in the heart of WT and *Nfix*-null mice, suggesting that no compensative mechanisms take place.

The proper functional pumping action of the heart is ensured by the consecutive and repetitive activation of different cardiac regions, the atria and the ventricles, whose rate of contraction is set by the spontaneous electrical activity of the SAN, the cardiac pacemaker. At the very beginning of heart development, the heartbeat originates from those cells/progenitors that will give rise to the adult SAN.[5] During all the embryonic developmental stages and also for few days postnatally, ventricular cells can also beat spontaneously, a characteristic that they lose in the first week or so. When we evaluated the expression of *Nfix* in the various cardiac regions of the adult heart, we found similar expression levels in adult atria and ventricles which, without an external stimulus, are normally quiescent, but found a significantly reduced expression in the SAN (Table 3). Interestingly, these data suggest an inverse correlation between *Nfix* levels and cardiomyocytes spontaneous beating rate. This observation is also strengthened by the fact that *Nfix* levels are much lower in spontaneously beating NRVC than in the AV (Table 3).

This evidence prompted us to investigate the functional role of *Nfix* downregulation on heart rate. We first evaluated the heart rate in vivo, in freely moving conscious WT and *Nfix*-null mice. As expected, we found physiological circadian fluctuations of the heart rate, which is significantly higher during the dark/active than during light/inactive phase.[10,20,21] Recent data clearly demonstrated that these fluctuations persist even after complete pharmacological block of both branches of the autonomic nervous system, and thus rate fluctuations are independent from autonomic modulation.[20,21]

TABLE 5 Action potential parameters analyzed in NRVC.

NRVCs	SCR, $n = 19$	Sh-*Nfix*, $n = 20$
RATE (bpm)	54.5 ± 9.0	57.8 ± 7.9*
MDP (mV)	−59.2 ± 1.7	−56.3 ± 2.3
APA (mV)	92.8 ± 3.0	92.6 ± 3.5
APD50c (ms)	107.7 ± 5.9	109.3 ± 7.1

*$p < 0.05$.

TABLE 6 I_{CaL} and I_f conductance in NRVC.

NRVC	I_{CaL} current		I_f current	
	SCR, $n = 5$	Sh-*Nfix*, $n = 9$	SCR, $n = 7$	Sh-*Nfix*, $n = 5$
g (pS/pF)	25.7 ± 3.8	39.7 ± 4.2*	44.83 ± 11.3	43.7 ± 9.1

*$p < 0.05$.

Here we show that *Nfix* null mice, present a significantly higher heart rate than WT littermates, independently of the light/dark phase of the day. Moreover, we found that the higher rate of *Nfix*-null mice is an intrinsic feature of the SAN, since the tachycardia persists in isolated SAN cardiomyocytes.

Interestingly, D'souza et al. have also shown that the circadian fluctuations of the spontaneous activity is intrinsic to SAN cells, remaining present after isolation (and thus denervation) of the tissue from the rest of the heart. Moreover, they demonstrated that rate differences are associated with a concomitant day/night fluctuation of HCN4 expression, the main isoform responsible (at mRNA, protein, and ion current levels) for the I_f current in the SAN.[20] We thus evaluated the expression level of the three main *Hcn* genes (*Hcn1*, *2* and *4*) expressed in the mouse SAN[22] and found that *Hcn4* mRNA was upregulated in *Nfix*-null SAN. However, functional analysis of the I_f current did not show any significant difference in the I_f current between WT and *Nfix*-null cells. This is however not surprising because changes in mRNA levels of *Hcn4* have been already shown to not correspond to changes in current amplitude. For example, we have recently shown that spontaneously beating hiPS-derived cardiomyocytes from patients with atrial fibrillation express significantly lower level of *HCN4*, than healthy controls, but have a significantly higher current density.[16] Similarly, SAN-like cells derived from mouse embryonic stem cells overexpressing miR-1 display similar levels of *Hcn4* but a significantly reduced I_f current.[17]

In order to investigate the molecular mechanism at the basis of the sinus tachycardia we analyzed expression levels of calcium channel genes known to participate to the setting of SAN rhythm.[14,23]

Although in the literature no data are available on the specific effect of *Cacna1d* overexpression in cardiomyocytes, genetic ablation of *Cacna1d* in mice induced sinus node bradycardia.[24] Moreover, an upregulation of I_{CaL} similar to that observed here, has been shown to induce tachycardia in spontaneously beating hiPS-derived cardiomyocytes.[16] In order to understand if the physiological role of *Nfix* downregulation is limited to the mouse SAN or represent a more general physiological control of heart rate, we employed NRVC, a spontaneously beating cell model often used for analyzing basic modulatory pathways involving autorhythmic cells.[25] *Nfix*-silenced NRVC displayed a significantly higher spontaneous rate than scramble-infected NRVC. Interestingly, also in these cells, the tachycardia was due to an increased I_{CaL} current density without any change in the pacemaker I_f current, suggesting that the same transcriptional mechanisms modulating cardiomyocyte automaticity are conserved in different species.

In conclusion, we have shown here, for the first time, a detailed analysis of *Nfix* expression during mouse cardiac development and its functional role in this organ. In the developing heart, *Nfix* expression grows linearly from E12.5, reaches a plateau around the first postnatal week and then remains highly expressed up to adulthood. Differently from its role in the skeletal muscle, the lack of *Nfix* does not impair the normal morphological development of the heart. Of note, *Nfix* expression is abundant in the quiescent working myocardium (atria and ventricles) while it is significantly less expressed in autorhythmic cells such as in the pacemaker SAN cardiomyocytes and in immature, spontaneously beating NRVCs. From a functional point of view, in the heart *Nfix* appears to have an important role in setting the physiological heart rate; indeed, both *Nfix*-null animals and sh-*Nfix* NRVC display a significant intrinsic tachycardia due to an upregulation of the I_{CaL} calcium current known to play a pivotal contribution to pacemaker activity.

ACKNOWLEDGMENTS

We acknowledge Prof. Richard M. Gronostajski for providing *Nfix*-null+/− mice (C57 BL6/1295).

FUNDING INFORMATION

This work was supported by the Association Française contre les Myopathies AFM-Telethon (grant number 20002) and the European Community, ERCStG2011 (RegeneratioNfix 280611) to GM.

CONFLICT OF INTEREST STATEMENT

None.

ORCID

Patrizia Benzoni https://orcid.org/0000-0002-3371-3301
Chiara Piantoni https://orcid.org/0000-0002-3621-8402
Luca Carnevali https://orcid.org/0000-0001-9053-7976
Mirko Baruscotti https://orcid.org/0000-0002-6155-8388
Andrea Barbuti https://orcid.org/0000-0002-4521-4913

REFERENCES

1. Piper M, Gronostajski R, Messina G. Nuclear factor one X in development and disease. *Trends Cell Biol*. 2019;29(1):20-30.
2. Messina G, Biressi S, Monteverde S, et al. Nfix regulates fetal-specific transcription in developing skeletal muscle. *Cell*. 2010;140(4):554-566.
3. Rossi G, Antonini S, Bonfanti C, et al. Nfix regulates temporal progression of muscle regeneration through modulation of myostatin expression. *Cell Rep*. 2016;14(9):2238-2249.
4. Chaudhry AZ, Lyons GE, Gronostajski RM. Expression patterns of the four nuclear factor I genes during mouse

embryogenesis indicate a potential role in development. *Dev Dyn*. 1997;208(3):313-325.
5. Barbuti A, Robinson RB. Stem cell-derived nodal-like cardiomyocytes as a novel pharmacologic tool: insights from sinoatrial node development and function. *Pharmacol Rev*. 2015;67(2):368-388.
6. Hoffmann S, Berger IM, Glaser A, et al. Islet1 is a direct transcriptional target of the homeodomain transcription factor Shox2 and rescues the Shox2-mediated bradycardia. *Basic Res Cardiol*. 2013;108(2):339.
7. Campbell CE, Piper M, Plachez C, et al. The transcription factor Nfix is essential for normal brain development. *BMC Dev Biol*. 2008;8:52.
8. Baruscotti M, Bucchi A, Viscomi C, et al. Deep bradycardia and heart block caused by inducible cardiac-specific knockout of the pacemaker channel gene Hcn4. *Proc Natl Acad Sci U S A*. 2011;108(4):1705-1710.
9. Sgoifo A, Stilli D, Medici D, Gallo P, Aimi B, Musso E. Electrode positioning for reliable telemetry ECG recordings during social stress in unrestrained rats. *Physiol Behav*. 1996;60(6):1397-1401.
10. Piantoni C, Carnevali L, Molla D, et al. Age-related changes in cardiac autonomic modulation and heart rate variability in mice. *Front Neurosci*. 2021;15:617698.
11. Avitabile D, Crespi A, Brioschi C, et al. Human cord blood CD34$^+$ progenitor cells acquire functional cardiac properties through a cell fusion process. *Am J Physiol Heart Circ Physiol*. 2011;300(5):H1875-H1884.
12. Bucchi A, Barbuti A, Difrancesco D, Baruscotti M. Funny current and cardiac rhythm: insights from HCN knockout and transgenic mouse models. *Front Physiol*. 2012;3:240.
13. DiFrancesco ML, Mesirca P, Bidaud I, Isbrandt D, Mangoni ME. The funny current in genetically modified mice. *Prog Biophys Mol Biol*. 2021;166:39-50.
14. Mangoni ME, Couette B, Bourinet E, et al. Functional role of L-type Cav1.3 Ca^{2+} channels in cardiac pacemaker activity. *Proc Natl Acad Sci U S A*. 2003;100(9):5543-5548.
15. Louradour J, Bortolotti O, Torre E, et al. L-type Ca(v)1.3 calcium channels are required for Beta-adrenergic triggered automaticity in dormant mouse sinoatrial pacemaker cells. *Cells*. 2022;11(7):1114. https://doi.org/10.3390/cells11071114
16. Benzoni P, Campostrini G, Landi S, et al. Human iPSC modelling of a familial form of atrial fibrillation reveals a gain of function of If and ICaL in patient-derived cardiomyocytes. *Cardiovasc Res*. 2020;116(6):1147-1160.
17. Benzoni P, Nava L, Giannetti F, et al. Dual role of miR-1 in the development and function of sinoatrial cells. *J Mol Cell Cardiol*. 2021;157:104-112.
18. Harris L, Genovesi LA, Gronostajski RM, Wainwright BJ, Piper M. Nuclear factor one transcription factors: divergent functions in developmental versus adult stem cell populations. *Dev Dyn*. 2015;244(3):227-238.
19. Akazawa H, Komuro I. Cardiac transcription factor Csx/Nkx2-5: its role in cardiac development and diseases. *Pharmacol Ther*. 2005;107(2):252-268.
20. D'Souza A, Wang Y, Anderson C, et al. A circadian clock in the sinus node mediates day-night rhythms in Hcn4 and heart rate. *Heart Rhythm*. 2021;18(5):801-810.
21. Barazi N, Polidovitch N, Debi R, Yakobov S, Lakin R, Backx PH. Dissecting the roles of the autonomic nervous system and physical activity on circadian heart rate fluctuations in mice. *Front Physiol*. 2021;12:692247.
22. Marionneau C, Couette B, Liu J, et al. Specific pattern of ionic channel gene expression associated with pacemaker activity in the mouse heart. *J Physiol*. 2005;562(Pt 1):223-234.
23. Christel CJ, Cardona N, Mesirca P, et al. Distinct localization and modulation of Cav1.2 and Cav1.3 L-type Ca^{2+} channels in mouse sinoatrial node. *J Physiol*. 2012;590(24):6327-6342.
24. Mesirca P, Torrente AG, Mangoni ME. Functional role of voltage gated Ca(2+) channels in heart automaticity. *Front Physiol*. 2015;6:19.
25. Campostrini G, Bonzanni M, Lissoni A, et al. The expression of the rare caveolin-3 variant T78M alters cardiac ion channels function and membrane excitability. *Cardiovasc Res*. 2017;113(10):1256-1265.

How to cite this article: Landi S, Giannetti F, Benzoni P, et al. Lack of the transcription factor *Nfix* causes tachycardia in mice sinus node and rats neonatal cardiomyocytes. *Acta Physiol*. 2023;00:e13981. doi:10.1111/apha.13981